

Calculation of Water-Exchange Rates on Aqueous Polynuclear Clusters and at Oxide–Water Interfaces

Jianwei Wang,[†] James R. Rustad,^{*,†} and William H. Casey^{*,†,‡}

Departments of Geology and of Chemistry, University of California, One Shields Avenue, Davis, California 95616

Received January 16, 2007

The rates of a wide variety of reactions in aqueous coordination compounds can be correlated with lifetimes of water molecules in the inner-coordination shell of the metal. For simple octahedral metal ions, these lifetimes span $\sim 10^{20}$ but are unknown, and experimentally inaccessible, for reactive sites in interfacial environments. Using recent data on nanometer-sized aqueous aluminum clusters, we show that lifetimes can be calculated from reactive-flux molecular dynamics simulations. Rates scale with the calculated metal–water bond lengths. Surprisingly, on all aluminum(III) mineral surface sites investigated, waters have lifetimes in the range of 10^{-8} – 10^{-10} s, making the surface sites as fast as the most reactive ions in the solution.

Water-exchange rates are key indicators of chemical reactivity in aqueous coordination compounds.¹ In the Eigen–Wilkins mechanism, for example, aqueous metal–ligand complexation reactions proceed via the rapid formation of an electrostatic ion pair, followed by slow elimination of a water molecule bound to the metal center. This latter step scales as the intrinsic water-exchange rate at the metal center. Once the rate of water detachment is known, the rates of other ligand-exchange reactions usually can be estimated to within a factor of 2–10.^{1b,c}

Rates of surface complexation reactions in environments characteristic of large aqueous polyoxocations and solid–water interfaces are intimately involved in diverse phenomena such as adsorption, electron transfer, and surface charging. There is no doubt that water-exchange rates are as fundamental to the reactivity of these systems as they are to coordination compounds, but, thus far, experimental determination of rates has been possible only for the simplest polynuclear systems.²

Here we use molecular dynamics calculations to estimate the water-exchange rates for a series of aluminum (oxy)-hydroxide compounds. These include the $\text{Al}(\text{H}_2\text{O})_6^{3+}$ monomer, the ϵ -Keggin ion $[\text{AlO}_4\text{Al}_{12}(\text{OH})_{24}(\text{H}_2\text{O})_{12}]^{7+/8+}$ (Al_{13}), the $[\text{Al}_2\text{O}_8\text{Al}_{28}(\text{OH})_{56}(\text{H}_2\text{O})_{26}]^{18+}$ (Al_{30}) aqueous polyoxocation, the surfaces of aluminum oxyhydroxide minerals boehmite (AlOOH) and gibbsite ($\text{Al}(\text{OH})_3$), and the aluminosilicate mineral kaolinite ($\text{Al}_2\text{Si}_2\text{O}_5(\text{OH})_4$) (Figure 1 and Table 1). For boehmite and gibbsite, five bridging oxygen atoms coordinate the metal centers. For gibbsite, the surface sites are coordinated to four oxo/hydroxo bridges and have one free hydroxyl. The surface terminations are unknown at the site-specific level and are offered here only as plausible representative structures. Like the minerals, the nanometer-sized polyoxocations (Al_{13} and Al_{30}) have waters bound at active sites that are separated by sets of relatively rigid hydroxyl bridges. In contrast to the mineral surfaces, the polyoxocations have active sites whose arrangements are known from X-ray diffraction studies on hydrated salts of these ions.³ The molecular dynamics calculations here tie these structurally diverse systems together into a simple structure–reactivity trend based on $\text{Al}-\text{OH}_2$ bond lengths and highlight the role of the Al_{13} and Al_{30} ions in systematically bridging the structural gap between the hexaquo ion and the oxide surfaces.

The $\text{Al}(\text{H}_2\text{O})_6^{3+}$ ion has the highest average charge per aluminum and should be the least reactive complex in the series. At 298 K, the $\text{Al}(\text{H}_2\text{O})_6^{3+}$ ion exchanges waters with a characteristic time τ^{298} of 1.2 s.^{1a} The 12 bound waters on the Al_{13} class of complexes are all equivalent and have $0.0009 \text{ s} < \tau^{298} < 0.005 \text{ s}$, depending on the identity of the central tetrahedral ion (aluminum, gallium, and germanium; cf. Figure 1a).² For Al_{30} , there are six distinct types of bound waters. Separate τ^{298} values cannot be assigned from the ^{17}O NMR experiments, although, in aggregate, the time scales are consistent with a few milliseconds to tenths of

* To whom correspondence should be addressed. E-mail: rustad@geology.ucdavis.edu (J.R.R.), whcasey@ucdavis.edu (W.H.C.).

[†] Department of Geology, University of California.

[‡] Department of Chemistry, University of California.

(1) (a) Helm, L.; Merbach, A. E. *Chem. Rev.* **2005**, *105*, 1923. (b) Richens, D. T. *The Chemistry of Aqua Ions*; John Wiley: New York, 1997. (c) Burgess, J. *Metal Ions in Solution*; John Wiley: London, 1978. (d) Richens, D. T. *Chem. Rev.* **2005**, *105*, 1961.

(2) (a) Casey, W. H. *Chem. Rev.* **2006**, *106*, 1. (b) Phillips, B. L.; Casey, W. H.; Karlsson, M. *Nature* **2000**, *404*, 379. (c) Phillips, B. L.; Lee, A.; Casey, W. H. *Geochim. Cosmochim. Acta* **2003**, *67*, 2725.

(3) (a) Allouche, L.; Gerardin, C.; Loiseau, T.; Ferey, G.; Taulelle, F. *Angew. Chem.* **2000**, *39*, 511. (b) Rowsell, J.; Nazar, L. F. *J. Am. Chem. Soc.* **2000**, *122*, 3777.

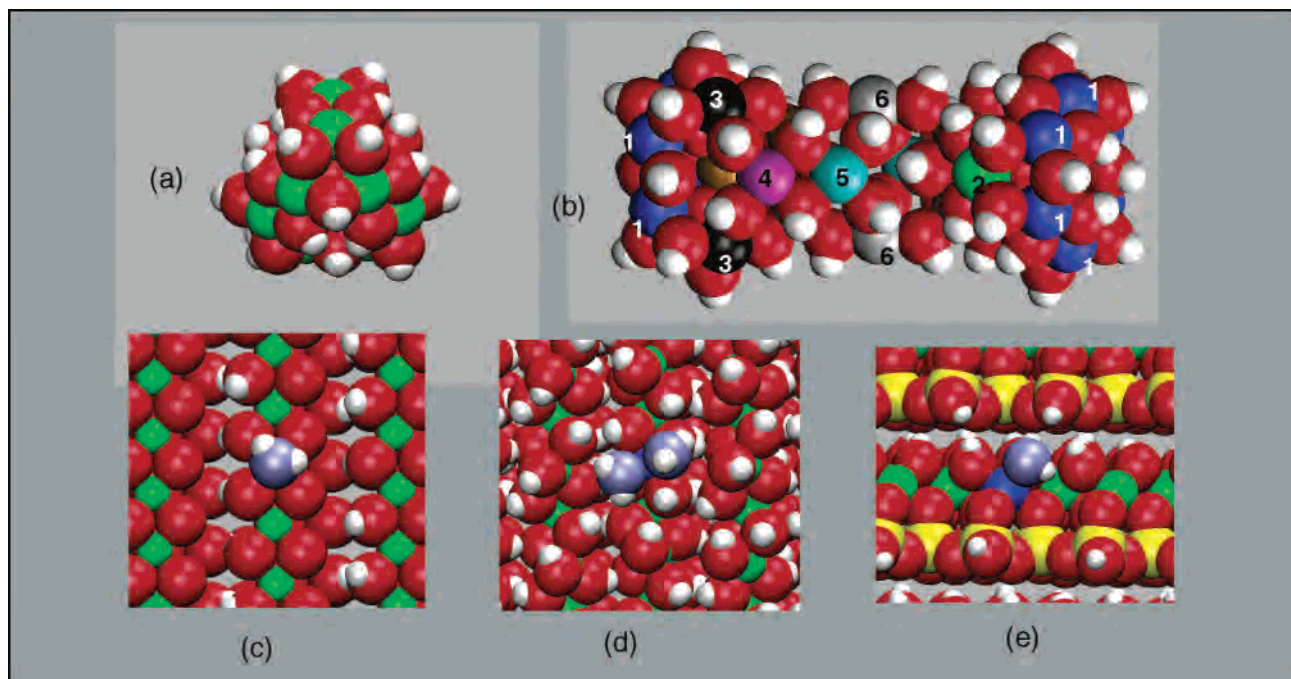


Figure 1. Aluminum(III) cationic clusters and mineral fragments used in these calculations. (a) The Al_{13} molecule is part of a class with stoichiometry $[\text{M}_4\text{Al}_{12}(\text{OH})_{24}(\text{H}_2\text{O})_{12}]^{7/8+}$ ($\text{M} = \text{Al}^{\text{III}}, \text{Ga}^{\text{III}}, \text{Ge}^{\text{IV}}$) and similar rates of solvent exchange from the 12 equivalent bound waters. (b) The Al_{30} $[\text{Al}_2\text{O}_8\text{Al}_{28}(\text{OH})_{56}(\text{H}_2\text{O})_{26}]^{18+}$ cation has six structurally distinct bound-water sites identified as S_1 – S_6 . (c) Boehmite $[\gamma\text{-AlOOH}]$ (001). (d) Gibbsite $[\alpha\text{-Al}(\text{OH})_3]$ (100). (e) Kaolinite $[\text{Al}_2\text{Si}_2\text{O}_5(\text{OH})_4]$ (1 $\bar{1}$ 0).

Table 1. Calculated Rates (at 300 K) and Activation Parameters for the Species in Figure 1^a

Site ($\langle \text{Al}-\text{OH}_2 \rangle$), Å	$\log k_{\text{TST}} (\text{s}^{-1})$	$\log \kappa$	$\log k (\text{s}^{-1})$	$\Delta H^\ddagger (\text{kJ}\cdot\text{mol}^{-1})$	$\Delta S^\ddagger (\text{J}\cdot\text{mol}^{-1}\cdot\text{K}^{-1})$
Al^{3+} 1.90 ^{exp} , 1.84 ^{calc}	−1.9	−1.0 ± 0.1	−2.9 ± 0.1 (0.08)	101.5 ± 0.25 (84.7 ± 3)	38 ± 7 (42 ± 9)
Al_{13} 1.92 ^{exp} , 1.92 ^{calc}	3.2	−2.3 ± 0.3	0.9 ± 0.3 (2.6 ± 0.4)	64.3 ± 1.4 (53 ± 12)	13 ± 4 (−7 ± 25)
Al_{30} S_1 , 1.93 ^{exp} , 1.98 ^{calc}	4.3	−2.4 ± 0.3	1.9 ± 0.3	58.0 ± 0.25	
Al_{30} S_2 , 1.93 ^{exp} , 1.99 ^{calc}	4.8	−1.6 ± 0.2	3.2 ± 0.2		
Al_{30} S_3 , 1.93 ^{exp} , 2.00 ^{calc}	4.7	−2.5 ± 0.4	2.2 ± 0.4		
Al_{30} S_4 , 1.88 ^{exp} , 1.94 ^{calc}	1.9	−2.3 ± 0.3	−0.4 ± 0.3	79.6 ± 1.7	
Al_{30} S_5 , 1.84 ^{exp} , 1.92 ^{calc}	2.0	−2.4 ± 0.3	−0.4 ± 0.3		
Al_{30} S_6 , 1.95 ^{exp} , 2.04 ^{calc}	7.5	−1.7 ± 0.2	5.8 ± 0.2	43.2 ± 4.3	21 ± 12
AlOOH	9.1	−1.2 ± 0.1	7.9 ± 0.1	17.7 ± 1.5	−34 ± 4
Al(OH) ₃	9.4	−0.5 ± 0.05	8.9 ± 0.05	19.8 ± 1.6	−18 ± 5
$\text{Al}_2\text{Si}_2\text{O}_5(\text{OH})_4$	10.3	−0.6 ± 0.05	9.7 ± 0.05	13.4 ± 1.9	−21 ± 6

^a Experimental values are listed in parentheses. Uncertainties are based on criteria discussed in the text. Bond lengths are from sources cited in refs 2, 3, and 8.

milliseconds.^{2d} Four of the bound waters, however, react so quickly that they could not be detected in ¹⁷O NMR, which means that they exchange at least a factor of 10 more rapidly than the others.

Molecular dynamics simulations were carried out on each of these species using the CLAYFF force field that operates in conjunction with the SPC/E water model and was developed for simulating aluminum hydroxide minerals and clays.⁴ For the Al_{13}^{7+} and Al_{30}^{18+} ions, charges on each of the aluminum ions were adjusted to reproduce the net charge on the complex (see the Supporting Information for GRO-MACS.top files).

The force field was implemented in the GROMACS molecular dynamics program.⁵ Water-exchange rates were calculated for each species using the reactive-flux method.⁶ In this method, an arbitrary reaction coordinate is expressed

between the outgoing/incoming water molecule and the aluminum site to which it is attached. The potential of mean force along the reaction coordinate, $W(r)$, was calculated using umbrella sampling, with 20–30 windows and a harmonic biasing potential. Individual windows are connected using the weighted histogram analysis technique.⁷

The rate constant is taken as $k_{\text{RF}} = \kappa k_{\text{TST}}$; k_{TST} is the transition-state rate constant calculated from $W(r)$:⁶

$$k_{\text{TST}} = \sqrt{\frac{1}{2\pi\mu\beta}} \frac{e^{-\beta W(r^\ddagger)}}{\int_0^{r^\ddagger} e^{-\beta W(r)} dr} \quad (1)$$

where the reaction coordinate r is the distance between the target metal ion and the exchanging water molecule, r^\ddagger is the position of the maximum in the $W(r)$, μ is the reduced mass (with respect to aluminum and water), and $\beta = 1/k_{\text{B}}T$. The transmission coefficient κ is obtained by starting a series of simulations ($\sim 10\,000$) with r constrained at r^\ddagger , integrating forward and backward in time and counting the fraction of

(4) Cygan, R. T.; Liang, J.-J.; Kalinichev, A. G. *J. Phys. Chem. B* **2004**, *108*, 1255.

(5) Lindahl, E.; Hess, B.; van der Spoel, D. *J. Mol. Model.* **2001**, *7*, 306.

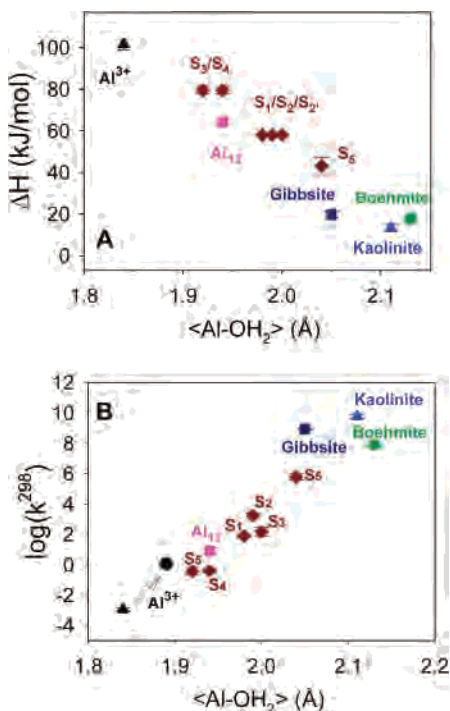


Figure 2. Activation enthalpies (A) and rate coefficients (B) correlated to calculated bond lengths. Rate coefficients for water exchange (s^{-1}) are estimated using eq 1 and transmission coefficients listed in Table 1.

successful barrier crossings. Contributions from k_{TST} and κ are given in Table 1 along with the calculated rates. Uncertainties in k_{TST} are taken from Monte Carlo bootstrap analysis.^{7b} The indicated errors in κ are given by regression of the number of successful barrier-crossing events versus time.

The calculated rates are in reasonable agreement with the measured rates and, as shown in Figure 2, correlate well with calculated Al–OH₂ bond lengths on the exchanging sites. Our calculated rate for the hexaquo ion is slow, consistent with the short bond length for the hexaquo complex by CLAYFF (1.83 Å [calcd] vs 1.90 Å [exptl]). Calculations on the Al₃₀ molecule reflect the site heterogeneity present in the Al₃₀ ion. The slowest rates are for the S₄ and S₅ sites, which have very short Al–OH₂ bond lengths both in the simulation and in the X-ray structure.³ The four symmetrically equivalent S₆ sites exchange much faster than the other sites, consistent with the experimental observation that four waters are too reactive to measure with ¹⁷O NMR.^{2d}

The temperature dependence of the rate constants was used to determine the activation parameters ΔH^\ddagger and ΔS^\ddagger (Figure 2). Activation parameters have been measured for both Al–(H₂O)₆³⁺ and Al₁₃. The calculated value of ΔH^\ddagger for the Al–(H₂O)₆³⁺ ion ($101.5 \pm 2.6 \text{ kJ}\cdot\text{mol}^{-1}$) is somewhat larger than the experimental value ($85 \pm 3 \text{ kJ}\cdot\text{mol}^{-1}$; Table 1), which again reflects the short <Al–OH₂> bond length predicted by CLAYFF. The ability of the umbrella-sampling approach to relate ΔH^\ddagger to both the reaction coordinate *and* its associated transmission coefficient provides information complementary the quantum mechanical studies, which completely neglect the transmission contribution.^{8,9} The relationship between ΔH^\ddagger and the temperature dependence of the exchange rate is much clearer in the umbrella-sampling reactive-flux approach. ΔH^\ddagger of $64 \text{ kJ}\cdot\text{mol}^{-1}$ calculated for the Al₁₃ ion agrees well with the experimental values of 53 ± 12 , 63 ± 7 , and $56 \pm 8 \text{ kJ}\cdot\text{mol}^{-1}$ for the Al₁₃, GaAl₁₂, and GeAl₁₂ ions, respectively.^{2b}

Overall, the estimates of τ^{298} for the aluminous minerals are surprisingly short, falling within the range of $\sim 10^{-8}$ – 10^{-10} s, close to those for alkali and alkaline-earth metal ions. Waters bound at the edges of the minerals will exchange rapidly with bulk waters and with other ligands. The fast rates for these surface sites are consistent with the long Al–OH₂ bond lengths and also follow the general trend that rates increase, and ΔH^\ddagger values decrease, with increasing size and decreasing charge per aluminum ion of the complex. Such large increases in reactivity with increased polymerization were anticipated,¹⁰ where it was shown that rates of ligand-exchange reactions in chromium(III) ions and oligomers increase exponentially with the OH/Cr ratio.

This framework provides, for the first time, a means for estimating kinetic parameters for sites at aqueous polynuclear ions and oxyhydroxide surfaces. This result is enormously important for environmental chemistry, where treatment of reactions at the aqueous–mineral interface is a long-standing problem. The structure–reactivity relationship presented here places the ligand-exchange properties of extended interfacial systems on a new quantitative footing.

Acknowledgment. Support for this research was from the National Science Foundation via Grant EAR 05015600 and from the U.S. Department of Energy via Grants DE-FG03-96ER 14629 and DE-FG03-02ER 15693.

Supporting Information Available: GROMACS.top files. This material is available free of charge via the Internet at <http://pubs.acs.org>.

IC070079+

- (6) (a) Hanggi, P.; Talkner, P.; Borkovec, M. *Rev. Mod. Phys.* **1990**, *62*, 251. (b) Chandler, D. In *Classical and quantum dynamics in condensed-phase systems*; Berne, B. J., Ciccotti, G., Coker, D. K., Eds.; World Scientific: Singapore, 1998; p 3. (c) Den Otter, W.; Briels, W. J. *J. Am. Chem. Soc.* **1998**, *120*, 13167. (d) Kerisit, S.; Parker, S. C. *J. Am. Chem. Soc.* **2004**, *126*, 10152. (e) Spångberg, D.; Rey, R.; Hynes, J. T.; Hermansson, K. *J. Phys. Chem. B* **2003**, *107*, 4470. (f) Rustad, J. R.; Stack, A. G. *J. Am. Chem. Soc.* **2006**, *128*, 14778.
- (7) (a) Kumar, S.; Rosenberg, J. M.; Bouzida, D.; Swendsen, R. H.; Kollman, P. A. *J. Comput. Chem.* **1992**, *13*, 1011. (b) WHAM and the error analysis was carried out using Alan Grossfield's WHAM software package [<http://dasher.wustl.edu/alan/wham>].

- (8) Rotzinger, F. *Chem. Rev.* **2005**, *105*, 2003.
- (9) Stack, A. G.; Rustad, J. R.; Casey, W. H. *J. Phys. Chem. B* **2005**, *109*, 23771.
- (10) Crimp, S. J.; Spiccia, L.; Krouse, H. R.; Swaddle, T. W. *Inorg. Chem.* **1994**, *33*, 465.